

Research Article

A Comparative Analysis of Self-Rectifying Turbines for the Mutriku Oscillating Water Column Energy Plant

Erlantz Otaola ¹, Aitor J. Garrido ², Jon Lekube,³ and Izaskun Garrido²

¹*Tecnalia Electric Aircraft, Tecnalia Research and Innovation, 20009 San Sebastian, Spain*

²*Automatic Control Group (ACG), Institute of Research and Development of Processes, Dept. Aut. Control and Systems Eng., University of the Basque Country (UPV/EHU), P^o Rafael Moreno 3, Bilbao 48013, Spain*

³*Promotion and Subsidies Area, Basque Energy Board (EVE), 48011 Bilbao, Spain*

Correspondence should be addressed to Erlantz Otaola; otaola06@gmail.com

Received 31 October 2018; Accepted 30 December 2018; Published 23 January 2019

Academic Editor: Marcin Mrugalski

Copyright © 2019 Erlantz Otaola et al. This is an open access article distributed under the Creative Commons Attribution License, which permits unrestricted use, distribution, and reproduction in any medium, provided the original work is properly cited.

Oscillating Water Column (OWC) based devices are arising as one of the most promising technologies for wave energy harnessing. However, the most widely used turbine comprising its power take-off (PTO) module, the Wells turbine, presents some drawbacks that require special attention. Notwithstanding different control strategies are being followed to overcome these issues; the use of other self-rectifying turbines could directly achieve this goal at the expense of some extra construction, maintenance, and operation costs. However, these newly developed turbines in turn show diverse behaviours that should be compared for each case. This paper aims to analyse this comparison for the Mutriku wave energy power plant.

1. Introduction

1.1. Energy Problem. An increase in the energy consumers' environmental awareness seems to be driving a decrease on the fossil fuels and nuclear fission consumption, currently the most used energy resources [1–3]. This realization is pressuring into pushing renewable energy technology and its sources beating out other nonrenewables [4–6], as the 2020 climate and energy package reflects [7]. Renewable energy evolves around the natural resources that provide practically inexhaustible amounts of energy [8], either through the massive latent energy or through regenerative capabilities within the human time-scale. The most studied renewable energies today are solar, wind, wave, hydraulic, biomass, geothermic, and tidal [9].

Delucchi and Jacobson state that the total energy requirements could be fulfilled from solar, wind, and wave energy [10–12]. However, wave energy has lagged behind, even though the power density analysis stands up for the opposite [4]. According to this concept, when solar radiation heats air masses to different temperatures, it forces them to move and thus creates wind. Therefore, wind pools solar energy

and increases the power density. In turn, the ocean allows transferring energy from the wind to mechanical energy within the waves. Through this principle, at about 15-degree latitude, where the sun radiation is of 0.17 kW/m², the wind power density rises to 0.58 kW/m² and the wave power density climbs up to 8.42 kW/m² [4].

Additionally, the power density increment of the waves means that a sudden sun radiation stop would not suppose a wave activity decrease until many hours later. Besides, the sun could have easily come back by then, generating new powerful waves. This makes wave energy a precious and available resource. An analysis of the wave energy available to be harnessed estimates an annual total production around 100,000 kWh, compared to the 16,000 kWh annual consumption [13].

Consequently, hundreds of patents have been developed all around the globe to harness wave energy [14, 15]. Their classification divides them into on-shore or off-shore devices [16]. On-shore machines are easily manufactured and maintained, but harness less energy and there are fewer locations for installation. Oscillating vanes [17], tapering canals [18], and oscillating wave column (OWC) [19] are the most



FIGURE 1: The OWC power plant of Mutriku.

widely used types. Off-shore devices quite often require to be affixed to the seabed and are not as developed as on-shore ones. Mighty Whale [20], Wave Dragon [21], Wave Plane [22], Pelamis [23], Archimedes [24], Wave Star [25], and Power Buoy [26] technologies are examples of such type of technology. Oscillating wave column technology is nowadays deemed as the most promising candidate, due to it having the largest development rate compared to the rest [27–29].

1.2. Background. An OWC-technology-based device converts wave energy into an oscillating air flow, which in turn makes a turbine rotate. With the turbine attached to a power induction generator, energy is harnessed [19]. It can be understood as two main subassemblies: the capture chamber and the power take-off (PTO) system.

The capture chamber [30] consists of a hollow structure with an aperture placed in such a way that it stays below the sea water level (SWL) regardless of the tide. This configuration allows the water in and out of the cavity, which compresses and decompresses the air inside the cavity as the waves enter and leave. The air pressure variation forces an upwards and downwards air stream.

This air stream acts upon the PTO system composed of a turbine and a power induction generator [31]. It flows through the turbine, forcing it to spin and generating a pressure drop as a result. The spin creates a torque that turns the generator. The oscillating airflow would make a common turbine spin in a different direction each time. To optimize the turbine for unidirectional movement, a valve-based rectifying system could be used [19] or, in a more straightforward way, self-rectifying turbines.

Based on this technology, the Basque Energy Board (EVE) has built a ground-breaking power plant known as NEREIDA MOWC [32] in the Basque town of Mutriku (Figure 1), which consists of 16 turbo-generator modules rated at 18.5 kWh each with self-rectifying turbines coupled to a DFIG generator. This power plant makes use of 5-blade Wells turbines from the series NACA00XX [33–35]. The

Wells turbine, invented by Alan A. Wells in 1976, is regarded as the first of its kind [33, 34, 36–38]. Its rotor is made up of a number of blades symmetric in the direction normal to the airflow, allowing the tangential force to keep constant regardless of the airflow direction, making them spin always in the same direction [39]. However, this symmetry presents an inherent drawback, the stalling effect, which makes the turbine stall when the airflow through the turbine goes over a certain value. This sharply drops the efficiency of the turbine [40, 41].

There are many methods oriented towards the solution of this issue [42–45]:

- (i) relief valves
- (ii) air valve control
- (iii) rotational speed control

Relief valves permit some airflow to be bypassed to reduce the incoming air stream into the turbine [5, 46].

Air valve control allows for the regulation of the airflow input to the turbine so that it never reaches the airflow limit value, thus avoiding the stall effect. Several control methods have been developed for this model, such as artificial-neural-networks-based controllers [47] or robust sliding-mode controllers [48], but PID type controller is still considered the most efficient one [49].

The turbine can also be prevented from stalling by controlling its rotational speed which involves accelerating the turbine to a sufficient speed (Figure 2). In this case, the slip of the DFIG generator is set to vary so that higher speeds can be reached [47, 50]. This approach tends to calculate the maximum pressure drop throughout the turbine without stalling to determine the slip of the DFIG and modify the turbine rotational speed [49] (Figure 3).

As it can be observed, solving the stalling effect requires sufficient control mechanisms. However, it could be avoided directly by using a turbine without this issue. This substitution would additionally allow the focus of the control only on increasing the torque output of the system. There are many turbines that have been developed since Wells was created which could yield promising results. Pitch-controlled Wells, impulse, and radial with pitch-controlled guide vanes and biradial turbines are compared to the Wells turbine installed in Mutriku throughout this paper.

2. Materials and Methods

2.1. Turbines Description. Pitch-controlled Wells turbines (Figure 4) consist of endowing the Wells turbine with the capability of modifying the pitch angle between two extreme angles, $\pm\gamma$, to convert the incoming airflow more efficiently into rotational motion [51]. This increase in efficiency stems from the ability to diminish the hysteresis of a vane due to the influence of the vanes in close proximity [52]. This turbine also enhances the performance when starting up or at low speeds [53], allowing reaching higher speeds in a shorter amount of time, a desirable feature in OWC-based devices [54].

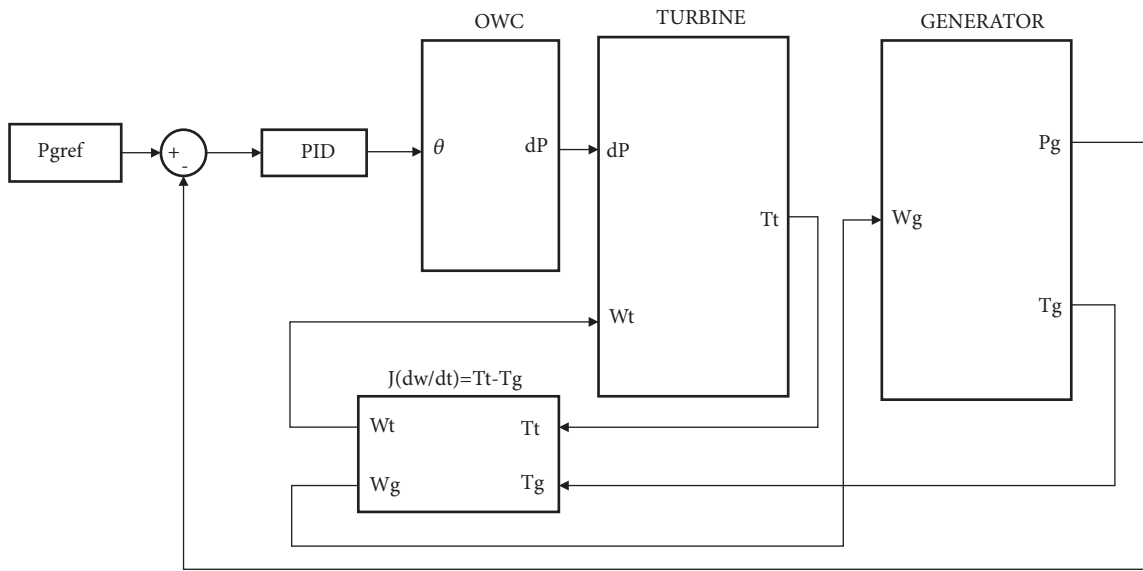


FIGURE 2: Rotational speed control diagram.

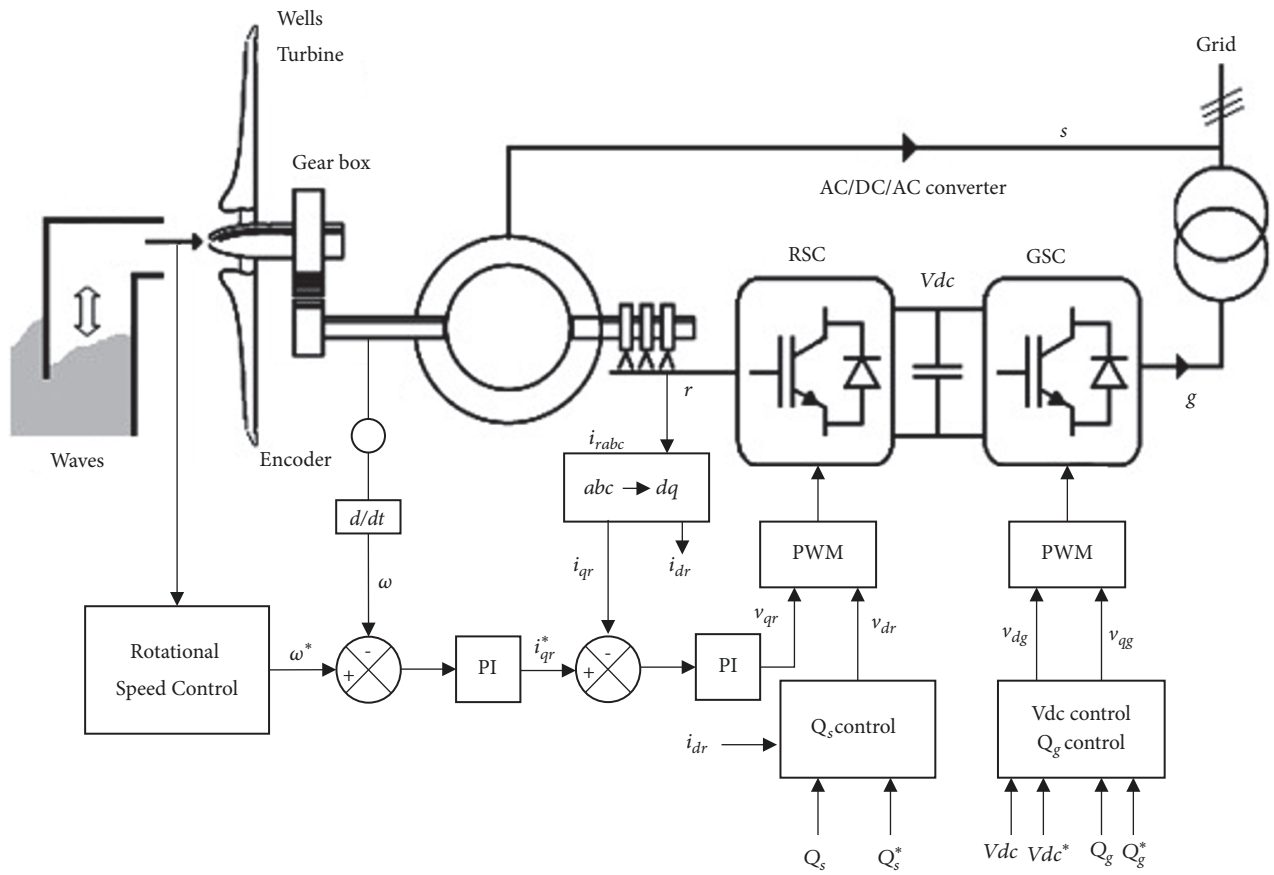


FIGURE 3: DFIG control strategy diagram.

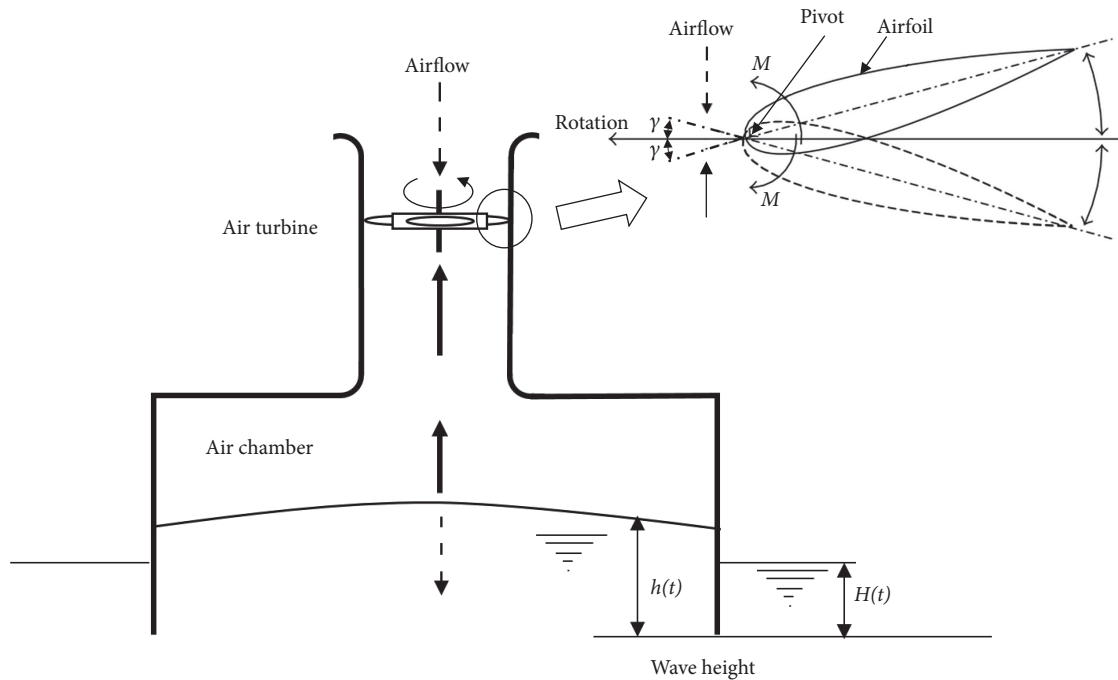


FIGURE 4: Wells turbine with pitch control.

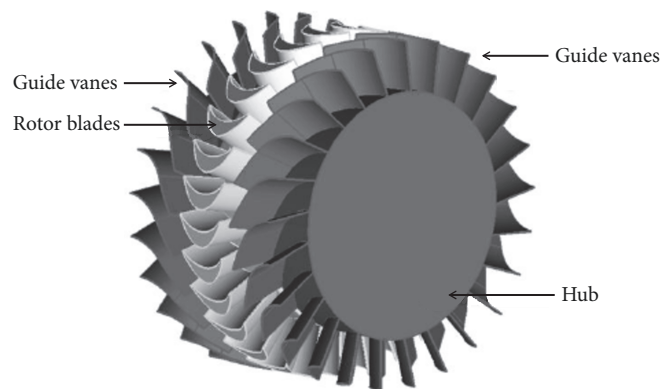


FIGURE 5: Impulse turbine.

Impulse turbines (Figure 5) solve the stalling problem, are capable of starting in a short period of time and of working at low speeds [55]. Setoguchi et al. [56–63] developed a variation of this turbine adding two rows of guide vanes, one upstream and other downstream, whose pitch is controlled to increase its efficiency. These guide vanes are mechanically coupled so that the one in the outgoing path does not obstruct the airflow when controlling the ingoing vane to optimize the energy conversion [64].

Radial turbines with pitch-controlled guide vanes (Figure 6) are similar to impulse turbines with the difference that the airflow enters the turbine radially and not axially [65–71]. They also include two rows of guide vanes, one upstream and other downstream, whose pitch is controlled between two extreme angles [70]. These turbines reduce the mechanical requirements of the impulse turbines but maintain all their benefits, such as the removal of the stall effect [72]. However,

the trade-off requires an extra system forcing the air in the radial direction.

Biradial turbines (Figure 7) are a new kind of a radially attacking turbine [73]. This turbine is also equipped with two rows of mechanically coupled guide vanes, which are axially displaced to guide the input airflow without obstructing the outgoing airflow. Obstructing the airflow would make the vanes stall [74]. Since these turbines use impulse-type vanes, all the drawbacks from the Wells turbines are solved. Additionally, their mechanical design allows them to convert wave energy more efficiently [73].

The data obtained by different sensors placed in the Mutriku wave power plant is used to compare these turbines, along with the Wells variant. From the data, inputs for the different turbine models can be created and therefore compute their outputs when subjected to the same inputs. This way, the most adequate turbine can be determined.

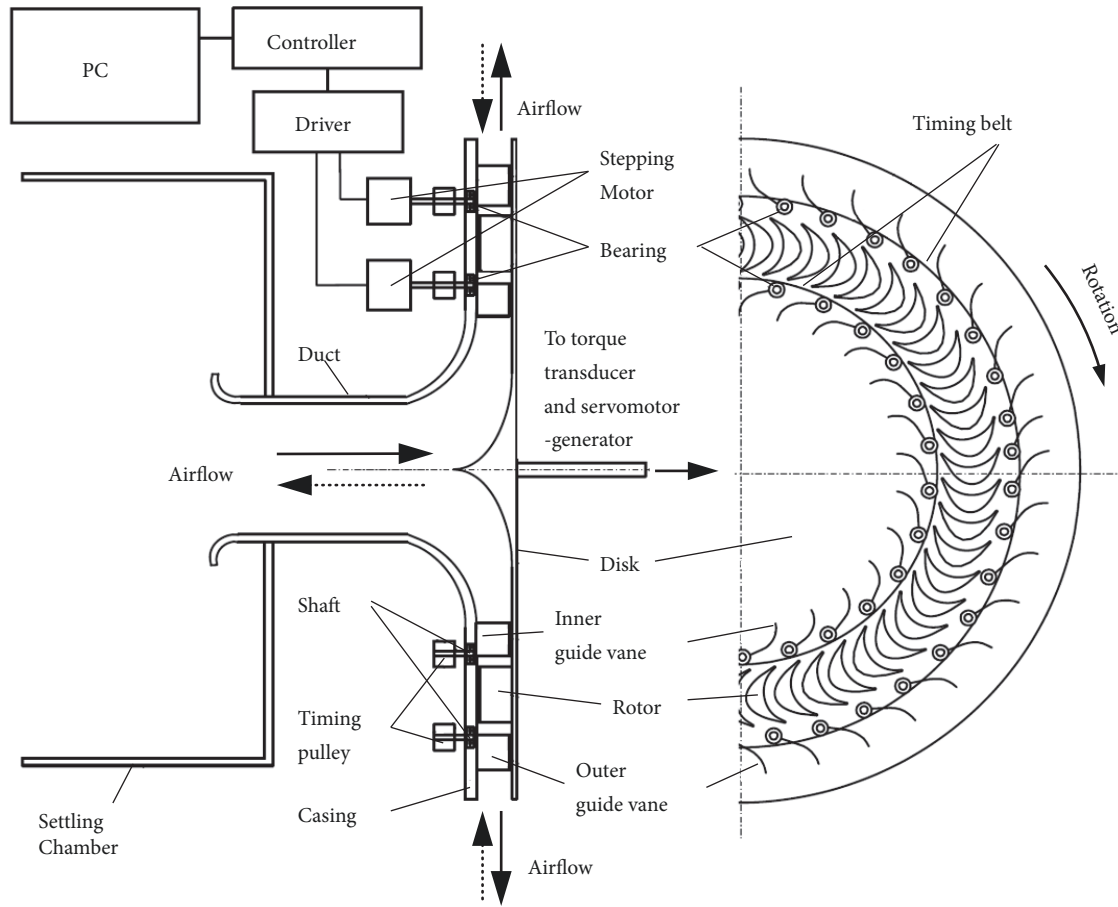


FIGURE 6: Radial turbine with pitch-controlled guide vanes.

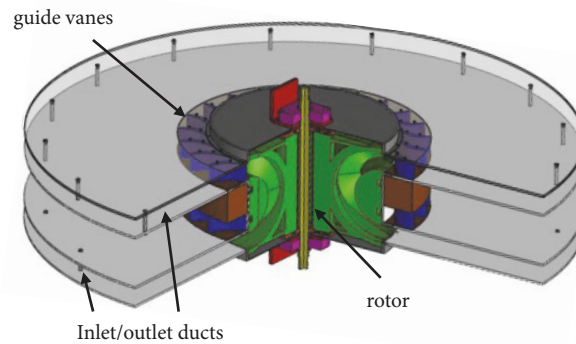


FIGURE 7: Biradial turbine.

2.2. *Sensors Description and Data Treatment.* The data used to simulate the environment and the control of the turbines comes from three different sources:

- (i) Basque Energy Board (EVE)
- (ii) AZTI-Tecnalia
- (iii) State harbours (website)

The following variables are provided by the EVE, from January 1st 2014 to May 15th 2014, with half second resolution:

- (i) Pressure (Pa)
- (ii) Air valve angle (degree)
- (iii) Rotational speed (rpm)
- (iv) System extracted power (kW)

From the aforementioned data, rotational speed and valve angle depend on the control strategy, whose parameters vary from one turbine to another. Therefore, these values depend

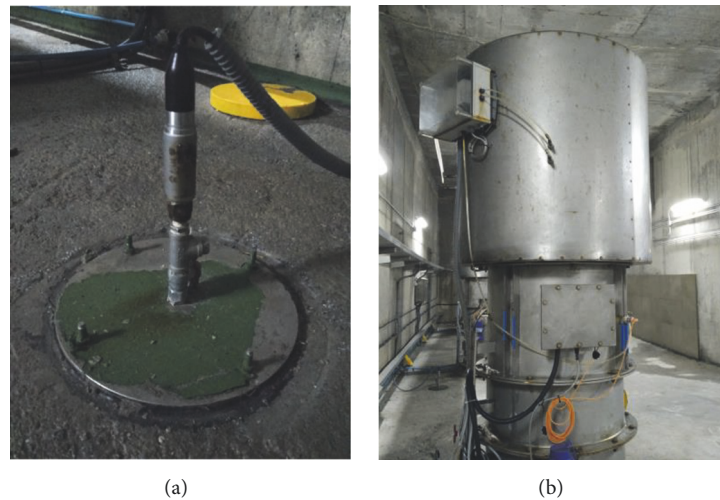


FIGURE 8: Pressure sensors in Mutriku. (a) Capture chamber static pressure sensor. (b) Pressure drop along the PTO sensor.

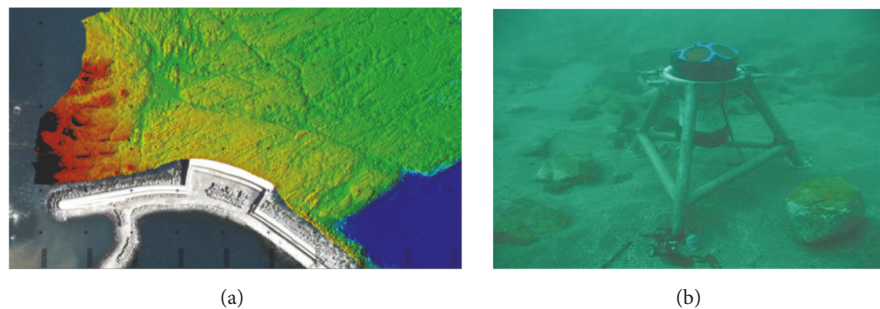


FIGURE 9: (a) Wave spectrum record. (b) RDI 600kHz.

on each turbine and the ones provided by the EVE are related to the Wells turbine use case.

The pressure and the extracted torque outputs are extensively used to compare against the outputs from the other turbines' models and hence determine the turbine whose response would best fit in Mutriku.

There are two types of pressure sensors in the power plant of Mutriku: one to measure the static pressure of the capture chamber and the other for the pressure drop along the turbo-generator module. The pressure of the capture chamber is measured by means of a *PTX 7355* type *Druck* sensor installed at the base of the power plant (Figure 8(a)). However, in order to obtain the pressure drop through the turbo-generator, two CMR controls P-sensors for low air pressure are employed, one at the inlet of the turbine and the second at the top of the turbo-generator module (Figure 8(b)) [75].

AZTI-Tecnalia provided the average height and period of the wave trains that took place during a period of 20 mins every 2 hours on May 12th 2014. From the wave fundamental parameters, two half-a-second resolutions vectors are generated, one for the amplitude and another for the period. Those vectors are used as inputs for all the models of the different turbines to objectively compare their response for the exact same conditions.

The sensor used to acquire this information is the Teledyne RDI 600kHz, an Acoustic Doppler Current Profiler (Figure 9).

This sensor measures water depth ranging from 0.7m to 90m. Laying in the seabed next to Mutriku, where the water depth is around 5m, this sensor allows measuring all the different wave heights. In order to harness the data, this can be done well via a serial/DC/computer cable well storing it in an internal memory card and then recovering it in the PC.

2.3. Turbine Models Development. The expression obtained in [76] to work out the pressure drop through the Wells turbine installed in Mutriku is a function of a parameter depending on the turbine itself, the power coefficient (C_a),

$$dp = C_a \frac{\rho b l_1 n}{2} \frac{1}{a_1} (v_t^2 + \omega_t^2 r^2), \quad (1)$$

The definition of this parameter may however vary from one turbine to another, making the expression of the pressure drop through the turbine change. Therefore, to make use of the previous unaltered expression, it is necessary to obtain an equation that relates the power coefficient in (1) to the power coefficient definition for each turbine.

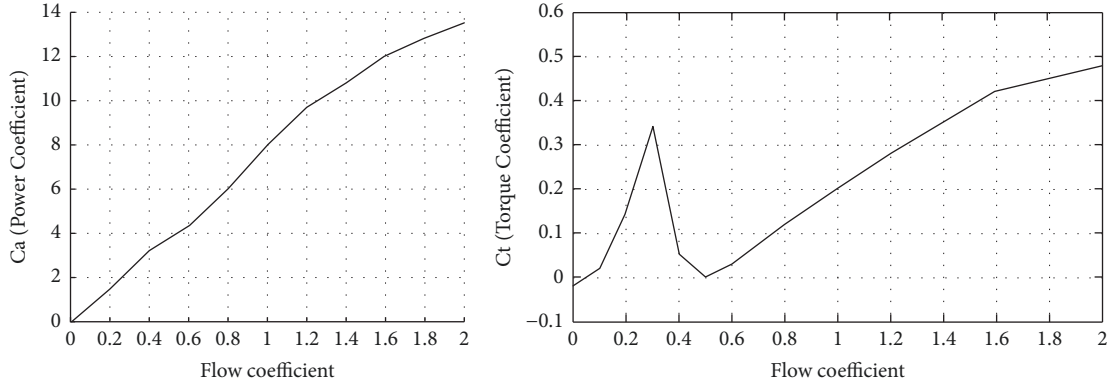


FIGURE 10: Relationship between flow coefficient-power coefficient and flow coefficient-torque coefficient.

Additionally, to benchmark the different turbines a comparison of the corresponding output torque directly linked to the output power is needed. According to [76], the output torque of the Wells turbine is defined as

$$T_t = \frac{dp \cdot C_t \cdot r \cdot a_1}{C_a} \quad (2)$$

Integrating (1) into (2), the output torque can also be defined as

$$T_t = C_t \frac{\rho b l_1 n}{2} r (v_t^2 + \omega_t^2 r^2) \quad (3)$$

This equation also depends on a coefficient of the turbine in use, the torque coefficient (C_t). Hence, as expected, this expression may differ from one turbine to another. Consequently, it is necessary to find an expression relating the torque coefficient in (3) and the torque coefficient for each turbine to compare.

Both previous parameters, power and torque coefficient, depend in turn on the flow coefficient, defined as

$$\Phi = \frac{v_t}{\omega_t r} \quad (4)$$

This definition may differ for some turbines, too. An expression relating this expression to the one defined for each turbine may thus also be necessary in those situations.

The relationships between flow coefficient and power coefficient and flow coefficient and torque coefficient relationships for the case of the Wells turbine are described in Figure 10.

In this sense, adapting the Wells turbine model for the case of Mutriku [76] to the different definitions of the torque coefficients, the pressure drop and output torque can be obtained for all the turbines and, therefore, determine which turbine would be the most appropriate for the case at Mutriku.

A convergence of the expressions for the different turbines is developed in the following way. The flow coefficients of the turbines to be compared are written as a function of the flow coefficient of the Wells turbine. The power and torque coefficients are in turn expressed reversely, writing the

TABLE 1: Parameters of the pitch-controlled Wells turbine.

Blade profile	NACA0021
Blade number	20
Cord length	75 mm
Solidity	0.75
Hub to tip ratio	0.7
Aspect ratio	0.6
Diameter	750 mm
Gap between rotor and casing	1 mm
Angle range	0-12°

coefficients for the Wells as a function of the coefficients of the new turbines.

This stems from the fact that the new turbines' expressions are integrated within a model devoted to the Wells. So to obtain the power or torque coefficients, the flow coefficient is used as an input. Therefore, once the flow coefficient (4) is calculated by the model for the different turbines, this serves as the input for the graph relating the flow coefficient to the other two (Figure 10 for the Wells turbine in Mutriku). Once the power and torque coefficients are obtained from the graphs, both are rewritten into the same form as the coefficients defined for the Wells turbine and then implemented in the model.

Pitch-Controlled Wells. The pitch-controlled Wells turbine analysed in this section is an adaptation to the duct diameter in Mutriku of the turbine defined in [54]. The main features of this turbine can be summarised in Table 1.

Regarding the turbine parameters, they are defined as

$$C_{a_{pW}} = \frac{dp_{pW} Q}{(\rho b l_1 v_a n (v_t^2 + \omega_t^2 r^2)) / 2}, \quad (5)$$

$$C_{t_{pW}} = \frac{T_{t_{pW}}}{(\rho b l_1 r n (v_t^2 + \omega_t^2 r^2)) / 2}, \quad (6)$$

$$\Phi_{pW} = \frac{v_t}{\omega_t r} \quad (7)$$

TABLE 2: Parameters of the biradial turbine.

Rotor	
Diameter	244 mm
Input/output width	53.7 mm
Blade number	3
Width	3.7 mm
Input/output angle	40°
Gap between rotor and casing	1 mm
Guide vanes	
Vane number	23
Geometry	Aerofoil
Rotor axis -vane distance	274 mm
Rotor end-vane distance	30 mm
Duct	
Diameter	750 mm

After a few modifications, it can be obtained that, for this turbine,

$$dp_{pW} = C_a \frac{\rho b l_1 n}{2} \frac{1}{a_1} (v_t^2 + \omega_t^2 r^2), \quad (8)$$

$$T_{t_{pW}} = C_t \frac{\rho b l_1 n}{2} r (v_t^2 + \omega_t^2 r^2) \quad (9)$$

Hence, the power and torque coefficient defined for this turbine can be directly used within the model developed for the Wells turbine [76] without further modifications.

Biradial. The biradial turbine analysed in this section is an adaptation to the duct diameter in Mutriku of the turbine described in [74]. The main features of this turbine can be summarised in Table 2.

Regarding the turbine parameters, they are defined as

$$C_{a_B} = \frac{dp_B}{\rho \omega_t^2 D^2} = \frac{dp_B}{4 \rho \omega_t^2 r^2}, \quad (10)$$

$$C_{t_B} = \frac{T_{t_B}}{\rho \omega_t^2 D^5}, \quad (11)$$

$$\Phi_B = \frac{Q}{\omega_t D^2} \quad (12)$$

It can be observed how all parameters vary with respect to the ones defined for the Wells turbine used in Mutriku. In this scenario, an expression to convert them into the type used in the Wells turbine model [76] must be worked out.

In the case of the power coefficient, (1) and (10) have been compared and, since the expression is equivalent,

$$dp = dp_B, \quad (13)$$

$$C_a \frac{\rho b l_1 n}{2} \frac{1}{a_1} (v_t^2 + \omega_t^2 r^2) = 4 C_{a_B} \cdot \rho \omega_t^2 r^2, \quad (14)$$

$$C_a = \frac{4 C_{a_B} \cdot \rho \omega_t^2 r^2 \cdot 2 a_1}{\rho b l_1 n (v_t^2 + \omega_t^2 r^2)}$$

$$C_a = C_{a_B} \cdot \frac{8 a_1}{b l_1 n (\Phi^2 + 1)} \quad (15)$$

In this way, once the power coefficient has been worked out via the graphs in [76], it is adequately transformed into the power coefficient defined for the Wells turbine by means of (15) so that it can be used in the pressure drop calculation.

Regarding the torque coefficient, since the torque output must be equal regardless of the equation used, (3) and (11) have to be compared and equal.

$$T_t = T_{t_B}, \quad (16)$$

$$C_t \frac{\rho b l_1 n}{2} r (v_t^2 + \omega_t^2 r^2) = C_{t_B} \rho \omega_t^2 D^5 = 32 C_{t_B} \rho \omega_t^2 r^5, \quad (17)$$

$$C_t = \frac{32 C_{t_B} \rho \omega_t^2 r^5 \cdot 2}{\rho b l_1 n r (v_t^2 + \omega_t^2 r^2)}$$

$$C_t = C_{t_B} \cdot \frac{64 r^2}{b l_1 n (\Phi^2 + 1)} \quad (18)$$

Analogous to the power coefficient, once the torque coefficient is determined, it is rewritten in an expression compatible with (3), which is then implemented in the model to obtain the output torque.

Finally, prior to the power and torque coefficient, the flow coefficient defined for the Wells turbine (implemented in the model) must be rewritten as a function of the type defined for the biradial (input of the graph). Therefore,

$$\begin{aligned} \Phi_B &= \frac{Q}{\omega_t D^3} = \frac{v_t a_1}{8 \omega_t r^3} = \frac{v_t \pi r^2}{8 \omega_t r^3} = \frac{v_t \pi}{8 \omega_t r} = \frac{\pi}{8} \frac{v_t}{\omega_t r} \\ &= \frac{\pi}{8} \Phi \end{aligned} \quad (19)$$

Now, all the necessary modifications have been obtained for the model to work properly for the Biradial, which is now ready for implementation.

Impulse. The impulse turbine analysed in this section is adapted to the duct diameter in Mutriku for the turbine defined in [64]. The main features of this turbine can be summarised in Table 3.

TABLE 3: Parameters of the impulse turbine.

Rotor	
Geometry	Circular arc ($r = 30.2$ mm) and ellipse
Cord length	54 mm
Edge radius	0.5 mm
Gap between rotor and casing	1 mm
Blade number	38
Radius	375 mm
Hub radius	210 mm
Angle	60°
Blade height	16.1 mm
Guide vanes	
Vane number	26
Stator	
Geometry	Straight line and circular arc ($r = 32$ mm)
Cord length	70 mm
Angle	15°

Regarding the turbine parameters, they are defined as

$$C_{a_i} = \frac{dp_I Q}{(\rho b l_1 v_a n (v_t^2 + \omega_t^2 r^2)) / 2}, \quad (20)$$

$$C_{t_i} = \frac{T_{t_i}}{(\rho b l_1 r n (v_t^2 + \omega_t^2 r^2)) / 2}, \quad (21)$$

$$\Phi_I = \frac{v_t}{\omega_t r} \quad (22)$$

After a few modifications, it can be obtained that, for this turbine,

$$dp_I = C_{a_i} \frac{\rho b l_1 n}{2} \frac{1}{a_1} (v_t^2 + \omega_t^2 r^2), \quad (23)$$

$$T_{t_i} = C_{t_i} \frac{\rho b l_1 n}{2} r (v_t^2 + \omega_t^2 r^2), \quad (24)$$

and, hence, that the power and torque coefficient defined for this turbine can be directly used within the model developed for the Wells turbine [76] without further modifications.

Radial with Pitch-Controlled Guide Vanes. The radial with pitch-controlled guide vanes turbine analysed in this section is adapted to the duct diameter in Mutriku for the turbine defined in [71]. The main features of this turbine can be summarised in Table 4.

TABLE 4: Parameters of the radial turbine.

Rotor	
Geometry	Circular arc ($r = 30.2$ mm) and ellipse
Cord length	54 mm
Edge radius	0.5 mm
Blade number	88
Radius	375 mm
Angle	60°
Solidity	2.02
Guide vanes	
Vane number	26
Stator	
Geometry	Straight line and circular arc ($r = 24.8$ mm)
Cord length	50 mm
Outer vane solidity	2.31
Inner vane solidity	2.29
Input angle	15°

Regarding the turbine parameters, they are defined as

$$C_{a_R} = \frac{dp_R}{(\rho (v_t^2 + \omega_t^2 r^2)) / 2}, \quad (25)$$

$$C_{t_R} = \frac{T_{t_R}}{(\rho a_1 r (v_t^2 + \omega_t^2 r^2)) / 2}, \quad (26)$$

$$\Phi_R = \frac{v_t}{\omega_t r} \quad (27)$$

It can be seen directly how the first two parameters, power and torque coefficient, vary with respect to the ones defined for the Wells turbine used in Mutriku. In this scenario, an expression to convert the previous two into the type used in the Wells turbine model [76] has to be worked out.

As in the biradial case, both output pressure and torque have to be the same regardless of the equation used to work it out. Equalling (1) and (25),

$$dp = dp_R, \quad (28)$$

$$C_a \frac{\rho b l_1 n}{2} \frac{1}{a_1} (v_t^2 + \omega_t^2 r^2) = C_{a_R} \cdot \frac{\rho}{2} (v_t^2 + \omega_t^2 r^2), \quad (29)$$

$$C_a = C_{a_R} \cdot \frac{a_1}{b l_1 n} \quad (30)$$

Equalling (3) and (26), the expression to modify the torque coefficient is obtained.

$$T = T_{t_R}, \quad (31)$$

$$C_t \frac{\rho b l_1 n}{2} r (v_t^2 + \omega_t^2 r^2) = C_{t_R} \cdot \frac{\rho a_1 r}{2} (v_t^2 + \omega_t^2 r^2), \quad (32)$$

$$C_t = C_{t_R} \cdot \frac{a_1}{b l_1 n} \quad (33)$$

Now, all the necessary modifications have been obtained for the model to work properly with the radial with pitch-controlled guide vanes turbine and the model is ready to be implemented.

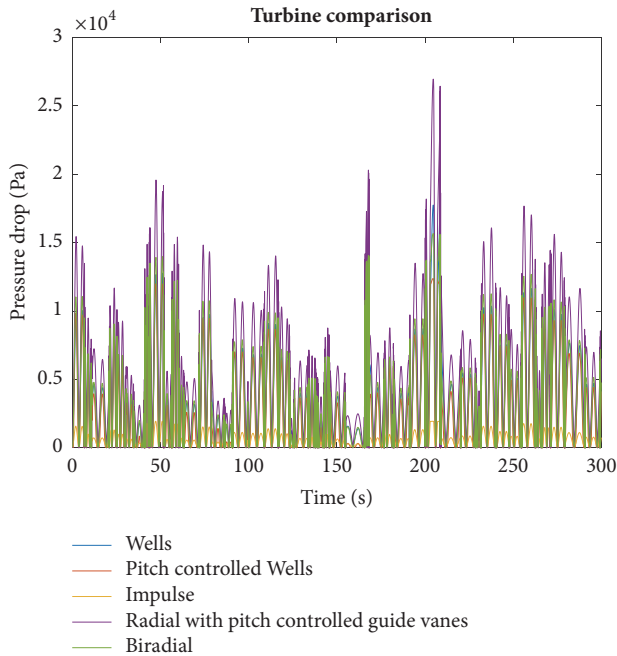


FIGURE 11: Model pressure drop output for the different turbines.

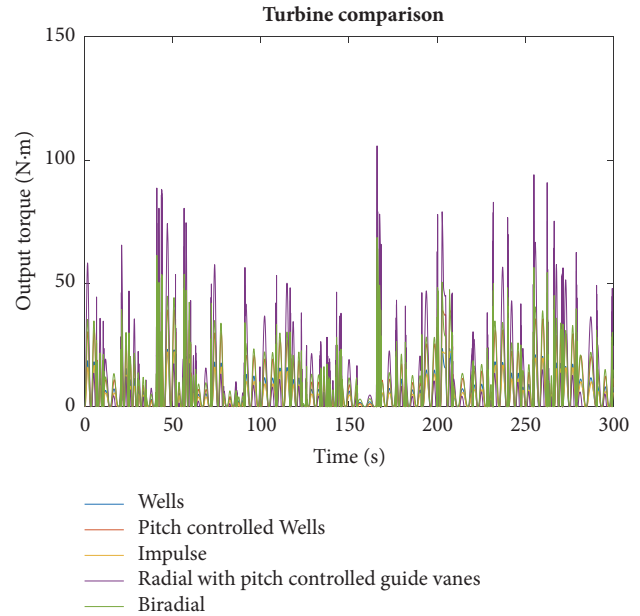


FIGURE 12: Model torque output for the different turbines.

3. Results

3.1. Models Modifications. In [76], a mathematical model was developed for the complete capture chamber of an OWC system including the turbine by determining both the pressure drop and the output torque of the turbine from the input wave parameters. For that, a Wells turbine was modelled and was validated with data from the Mutriku facility where a Wells turbine is installed. Then, [75] integrated this partial model into a complete wave-to-grid model. This complete model allowed modifying the control strategy obtaining the pressure drop and output torque for each control case study and thus implementing a control strategy to make the most of each turbine. Comparing the output torque of each turbine, the most adequate one can be chosen.

Taking that into account, the part of the model regarding the capture chamber along with the expressions obtained in the previous section, the turbine equation can be rewritten to suit the different definitions of flow, power, and torque coefficients whenever these modifications are needed, as in the case of the biradial and the radial with pitch-controlled guide vanes.

For pitch-controlled Wells and impulse turbines, each of them has proven that no expression modifications are needed. Therefore, only power and torque coefficients curves for each turbine have to be modified.

3.2. Models Outputs. Once the models are ready, the data in Section 2.1 is used to run the models and determine the pressure drop and output torque for the five studied turbines. Besides, the parameters of the turbines, such as radius and cord length are obtained from the turbines' data presented in Section 2.2.

This way, every turbine is tested within the exact same test environment (same wave parameters and same capture chamber geometry) but with its own attributes (turbine geometry and optimized control parameters). This allows for a comparison the response of the turbines in an unbiased way, thus extracting the most accurate conclusions when it comes to determining the most appropriate turbine for the case of Mutriku.

The pressure drop and output torque for the different turbines are as shown in Figures 11 and 12.

As it can be outlined from the previous figures, according to the pressure drop the radial turbine with pitch-controlled guide vanes seems to be the most appropriate for the case of Mutriku, for its pressure values exceed all others. Impulse turbines are the ones with the lowest pressure drop and therefore it seems not to be a well suited turbine for Mutriku.

However, this way to choose the most suitable turbine is regarding the output power that the turbine can provide, a feature related to the output torque that the turbine applies on the generator over time. Therefore, analysing the output torque of each turbine allows for the election of the one that provides the highest torque for the case of Mutriku disregarding the cost of manufacture, maintenance, and operation. Besides, even though the biradial turbine seems to provide the largest output torque, some uncertainty exists because the radial turbine presents the greatest peak value. Therefore, a more thorough analysis may be necessary, to work out the mean output torque, since this variable is one decisive feature to determine the best turbine for this case study (Table 5).

From the results above, the biradial turbine is deemed the most suitable option for the Mutriku wave power plant installation when considering only the output torque. It generates the largest pressure drop and mean output torque,

TABLE 5: Output torque mean values.

Wells	4.9428
Wells with pitch control	8.1732
Impulse	4.1148
Radial with pitch controlled guide vanes	7.0273
Biradial	9.7282

a 136% above the one that provides the lowest torque and a 19% above the second one, the Wells turbine with pitch control. This leaves the radial turbine with pitch-controlled guide vanes in the third place. Finally, Wells turbine and impulse turbine lag behind with results close to the others.

4. Conclusions

The results obtained throughout the present paper show how new self-rectifying turbines invented along the recent past years since the Wells invention have suffered an enormous enhancement. This upgrade has provided not only OWC technology-based power plants with a larger energy harnessing capability, but also additional benefits such as a slighter computational load since the stall effect control is avoided. This former fact allows for the development of more complex control algorithms that result in an increase of the amount of energy harnessed from the waves.

This way, it is evinced how, even if the current trends are prone to relate all the upcoming upgrades of OWC technology-based devices to software advancement, research on mechanical components shows how mechanical parts, such as self-rectifying turbines, also play an important role in it. This fact stands up for making progress on both research branches in parallel, one feeding the other, to achieve a faster, more advantageous, and more successful evolution of OWC technology-based devices.

Besides, this article is proof of how the model-based methodology is a good choice when carrying out analytic studies both of controllers and mechanical components and so. Following this approach, adapting the turbine model and adjusting the control for the particularities for each turbine, a systematic comparative analysis procedure has been performed for the different turbines in a reliable and low-cost effective manner.

Nomenclature

a : Wave amplitude
 a_1 : Capture chamber area
 b : Blade's height
 c : Wave propagation speed
 C_a : Power coefficient
 C_t : Torque coefficient
 dp : Pressure drop
 D : Diameter of the duct
 l : Length of the capture chamber
 l_1 : Length of blade's chord
 n : Number of blades
 Q : Air flow

r : Turbine's mean diameter
 t : Time variable
 T : Wave period
 T_t : Output torque
 v_t : Airflow linear speed
 ω : Wave angular frequency
 ω_t : Turbine rotation speed
 x : Space variable
 y : Wave instantaneous height
 λ : Wavelength
 ρ : Air density
 ϕ : Flow coefficient

Superscripts

B: Biradial turbine
 I: Impulse turbine
 R: Radial turbine with pitch-controlled guide vanes
 pW: Pitch-controlled Wells turbine.

Data Availability

The data used to support the findings of this study are available from the corresponding author upon request.

Conflicts of Interest

The authors declare that there are no conflicts of interest regarding the publication of this article.

Acknowledgments

This work was supported by the MINECO through the Research Project DPI2015-70075-R (MINECO/FEDER, UE) and in part by the University of the Basque Country (UPV/EHU) through PPG17/33. The authors would like to thank the collaboration of the Basque Energy Agency (EVE) through Agreement UPV/EHUEVE23/6/2011, the Spanish National Fusion Laboratory (EURATOM-CIEMAT) through Agreement UPV/EHUCIEMAT08/190, and EUSKAMPUS-Campus of International Excellence.

References

- [1] I. Garrido, A. J. Garrido, J. A. Romero, E. Carrascal, G. Sevillano-Berasategui, and O. Barambones, "Low effort L_i nuclear fusion plasma control using model predictive control laws," *Mathematical Problems in Engineering*, vol. 2015, Article ID 527420, 8 pages, 2015.
- [2] I. Garrido, A. J. Garrido, M. G. Sevillano, and J. A. Romero, "Robust Sliding Mode Control for Tokamaks," *Mathematical Problems in Engineering*, vol. 2012, Article ID 341405, 14 pages, 2012.
- [3] A. J. Garrido, I. Garrido, O. Barambones, P. Alkorta, and F. J. Maseda, "Simple linear models for plasma control in tokamak reactors," in *Proceedings of the 2008 International Conference on Control, Automation and Systems, (ICCAS '08)*, pp. 2429–2432, 2008.

- [4] J. Lekube, A. J. Garrido, I. Garrido, and E. Otaola, "Output power improvement in oscillating water column-based wave power plants," *Revista Iberoamericana de Automatica e Informatica Industrial*, vol. 15, no. 2, pp. 145–155, 2018.
- [5] A. J. Garrido, I. Garrido, M. Amundarain, M. Alberdi, and M. De La Sen, "Sliding-mode control of wave power generation plants," *IEEE Transactions on Industry Applications*, vol. 48, no. 6, pp. 2372–2381, 2012.
- [6] I. Garrido, A. J. Garrido, M. Alberdi, M. Amundarain, and O. Barambones, "Performance of an ocean energy conversion system with DFIG sensorless control," *Mathematical Problems in Engineering*, vol. 2013, Article ID 260514, 14 pages, 2013.
- [7] Ministerio de Agricultura, Alimentación y Medio Ambiente, "Paquete de Energía y Cambio Climático 2013-2020". Available in: <http://www.magrama.gob.es/es/cambio-climatico/temas/el-proceso-internacional-de-lucha-contra-el-cambio-climatico/la-union-europea/>.
- [8] Intergovernmental Panel on Climate Change, "Renewable Energy Sources and Climate Change Mitigation". Available in: http://srren.ipcc-wg3.de/report/IPCC_SRREN_Full_Report.pdf.
- [9] F. Fusco, G. Nolan, and J. V. Ringwood, "Variability reduction through optimal combination of wind/wave resources - An Irish case study," *Energy*, vol. 35, no. 1, pp. 314–325, 2009.
- [10] M. Delucchi, "Wind, water and solar power for the world," *IEEE Spectrum*, 2011.
- [11] M. Z. Jacobson and M. A. Delucchi, "Providing all global energy with wind, water, and solar power, part I: technologies, energy resources, quantities and areas of infrastructure, and materials," *Energy Policy*, vol. 39, no. 3, pp. 1154–1169, 2011.
- [12] M. Z. Jacobson and M. A. Delucchi, "Providing all global energy with wind, water, and solar power, part II: reliability, system and transmission costs, and policies," *Energy Policy*, vol. 39, no. 3, pp. 1170–1190, 2011.
- [13] European Ocean Energy Association, 2013 Industry Vision Paper. Available in: http://www.oceanenergy-europe.eu/images/Publications/European_Ocean_Energy-Industry_Vision_Paper_2013.pdf (last accessed April 2015).
- [14] D. Y. Goswami and F. Kreith, *Energy Conversion*, CRC Press, 2007.
- [15] H. Polinder and M. Scuotto, "Wave energy converters and their impact on power systems," in *Proceedings of the 2005 International Conference on Future Power Systems*, pp. 62–70, Amsterdam, The Netherlands, November 2005.
- [16] J. A. Carta González, R. Calero Pérez, A. Colmenar Santos, and M. A. Castro Gil, "Clasificación de los dispositivos de captación," in *Centrales de energías renovables: Generación eléctrica con energías renovables*, pp. 586–604, Madrid, España: Pearson Educación, 1st edition, 2009.
- [17] J. A. Carta González, R. Calero Pérez, A. Colmenar Santos, and M. A. Castro Gil, "Los alerones oscilantes," in *Centrales de energías renovables: Generación eléctrica con energías renovables*, pp. 593–594, Madrid, España: Pearson Educación, 1st edition, 2009.
- [18] J. A. Carta González, R. Calero Pérez, A. Colmenar Santos, and M. A. Castro Gil, "Los canales ahusados," in *Centrales de energías renovables: Generación eléctrica con energías renovables*, pp. 594–595, Madrid, España: Pearson Educación, 1st edition, 2009.
- [19] J. A. Carta González, R. Calero Pérez, A. Colmenar Santos, and M. A. Castro Gil, "Las columnas oscilantes de agua (OWC)," in *Centrales de energías renovables: Generación eléctrica con energías renovables*, pp. 588–593, Madrid, España: Pearson Educación, 1st edition, 2009.
- [20] J. A. Carta González, R. Calero Pérez, A. Colmenar Santos, and M. A. Castro Gil, "Mighty Whale (Poderosa Ballena)," in *Centrales de energías renovables: Generación eléctrica con energías renovables*, pp. 596–597, Madrid, España: Pearson Educación, 1st edition, 2009.
- [21] J. A. Carta González, R. Calero Pérez, A. Colmenar Santos, and M. A. Castro Gil, "Wave Dragon (Dragón de olas)," in *Centrales de energías renovables: Generación eléctrica con energías renovables*, pp. 597–598, Madrid, España: Pearson Educación, 1st edition, 2009.
- [22] J. A. Carta González, R. Calero Pérez, A. Colmenar Santos et al., "WavePlane (Plano de olas)," in *Centrales de energías renovables: Generación eléctrica con energías renovables*, pp. 598–600, Madrid, España: Pearson Educación, 1st edition, 2009.
- [23] J. A. Carta González, R. Calero Pérez, A. Colmenar Santos et al., "Pelamis," in *Centrales de energías renovables: Generación eléctrica con energías renovables*, pp. 600–601, Madrid, España: Pearson Educación, 1st edition, 2009.
- [24] J. A. Carta González, R. Calero Pérez, A. Colmenar Santos et al., "Archimedes," in *Centrales de energías renovables: Generación eléctrica con energías renovables*, p. 601, Madrid, España: Pearson Educación, 1st edition, 2009.
- [25] J. A. Carta González, R. Calero Pérez, A. Colmenar Santos et al., "Wave Star (Estrella de las olas)," in *Centrales de energías renovables: Generación eléctrica con energías renovables*, pp. 601–603, Madrid, España: Pearson Educación, 1st edition, 2009.
- [26] J. A. Carta González, R. Calero Pérez, A. Colmenar Santos et al., "PowerBuoy," in *Centrales de energías renovables: Generación eléctrica con energías renovables*, pp. 603–604, Madrid, España: Pearson Educación, 1st edition, 2009.
- [27] M. A. Ormaza, M. A. Goitia, A. J. G. Hernández, I. G. Hernández et al., "Neural control of the Wells turbine-generator module," in *Proceedings of the 2009 IEEE Conference on Decision and Control*, pp. 7315–7320, IEEE, 2009.
- [28] M. de la Sen, A. J. Garrido, J. C. Soto, O. Barambones, and I. Garrido, "Suboptimal Regulation of a Class of Bilinear Interconnected Systems with Finite-Time Sliding Planning Horizons," *Mathematical Problems in Engineering*, vol. 2008, Article ID 817063, 26 pages, 2008.
- [29] A. J. Garrido, I. Garrido, M. Alberdi, M. Amundarain, O. Barambones, and J. A. Romero, "Robust control of oscillating water column (OWC) devices: Power generation improvement," *OCEANS 2013 MTS/IEEE - San Diego: An Ocean in Common*, art. no. 6740982, 2013.
- [30] Y. Torre-Encino, I. Ortubia, de López Aguilera, and L. I. J. Marqués, "Mutriku wave power plant: From the thinking out the reality," in *Proceedings of 8th European Wave Tidal Energy Conference*, pp. 319–329, 2009.
- [31] A. El Marjani, F. Castro Ruiz, M. A. Rodriguez, and M. T. Parra Santos, "Numerical modelling in wave energy conversion systems," *Energy*, vol. 33, no. 8, pp. 1246–1253, 2008.
- [32] Y. Torre-Encino, "Mutriku Wave Power Plant: From Conception to Reality," in *European Federation Of Regional Energy and Environmental Agencies (FEDARENE)*, Brussels, Belgium, 2009.
- [33] T. Setoguchi and M. Takao, "Current status of self rectifying air turbines for wave energy conversion," *Energy Conversion and Management*, vol. 47, no. 15–16, pp. 2382–2396, 2006.

- [34] S. Raghunathan, "Performance of the Wells self-rectifying turbine," *The Aeronautical Journal*, vol. 89, no. 890, pp. 369–379, 1985.
- [35] V. Jayashankar, S. Anand, T. Geetha et al., "A twin unidirectional impulse turbine topology for OWC based wave energy plants," *Journal of Renewable Energy*, vol. 34, no. 3, pp. 692–698, 2009.
- [36] L. Gato and V. Warfield, "Performance of a high-solidity Wells turbine for an OWC wave power plant," in *Proceedings of the European Wave Energy Symposium*, pp. 181–190, 1994.
- [37] M. Inoue, K. Kaneko, T. Setoguchi, and T. Saruwatari, "Studies on the Wells Turbine for Wave Power Generator (Turbine Characteristics and Design Parameter for Irregular Wave)," *JSME International Journal*, vol. 31, no. 4, pp. 676–682, 1988.
- [38] S. Shaaban, "Insight analysis of biplane wells turbine performance," *Energy Conversion and Management*, vol. 59, pp. 50–57, 2012.
- [39] A. Thakker and R. Abdulhadi, "Effect of blade profile on the performance of wells turbine under unidirectional sinusoidal and real sea flow conditions," *International Journal of Rotating Machinery*, vol. 2007, Article ID 51598, 9 pages, 2007.
- [40] V. Jayashankar, S. Anand, T. Geetha et al., "A twin unidirectional impulse turbine topology for OWC based wave energy plants," *Journal of Renewable Energy*, vol. 34, no. 3, pp. 692–698, 2008.
- [41] S. Raghunathan, T. Setoguchi, and K. Kaneko, "The wells air turbine subjected to inlet flow distortion and high levels of turbulence," *International Journal of Heat and Fluid Flow*, vol. 8, no. 2, pp. 165–167, 1987.
- [42] J. Klamka, "Controllability and minimum energy control of linear fractional discrete-time infinite-dimensional systems," in *Proceedings of the 11th IEEE International Conference on Control & Automation*, vol. 162, pp. 1210–1214, Taichung, Taiwan.
- [43] A. Babiarz et al., "Controllability of discrete-time linear switched systems with constrains on switching signal," in *Proceedings of the 7th Asian Conference on Intelligent Information and Database Systems (ACIIDS '15)*, vol. 9011, Part I of *Lecture Notes in Artificial Intelligence*, pp. 304–312, Bali, Indonesia, 2015.
- [44] A. Czornik and M. Niezabitowski, "Alternative formulae for lower general exponent of discrete linear time-varying systems," *Journal of The Franklin Institute*, vol. 352, no. 1, pp. 399–419, 2015.
- [45] J. Klamka et al., "Trajectory controllability of semilinear systems with delay," in *Proceedings of the 7th Asian Conference on Intelligent Information and Database Systems (ACIIDS '15)*, vol. 9011, Part I of *Lecture Notes in Artificial Intelligence*, pp. 313–323, Bali, Indonesia, 2015.
- [46] A. F. D. O. Falcao, L. C. Vieira, P. A. P. Justino, and J. M. C. S. André, "By-pass air-valve control of an OWC wave power plant," *Journal of Offshore Mechanics and Arctic Engineering*, vol. 125, no. 3, pp. 205–210, 2003.
- [47] M. Amundarain, M. Alberdi, A. J. Garrido, and I. Garrido, "Neural control of the Wells turbine-generator module," in *Proceedings of the 48th IEEE Conference on Decision and Control*, pp. 7315–7320, 2009.
- [48] O. Barambones and A. J. Garrido, "Adaptive sensorless robust control of AC drives based on sliding mode control theory," *International Journal of Robust and Nonlinear Control*, vol. 17, no. 9, pp. 862–879, 2007.
- [49] M. Amundarain, M. Alberdi, A. J. Garrido, and I. Garrido, "Modeling and simulation of wave energy generation plants: Output power control," *IEEE Transactions on Industrial Electronics*, vol. 58, no. 1, pp. 105–117, 2011.
- [50] V. Jayashankar, K. Udayakumar, B. Karthikeyan, K. Manivanan, N. Venkatraman, and S. Rangaprasad, "Maximizing power output from a wave energy plant," in *Proceedings of the IEEE Power Engineering Society Winter Meeting*, vol. 3, pp. 1796–1801, 2000.
- [51] T. Setoguchi et al., "Air-Turbine with Self-Pitch-Controlled Blades for Wave Energy Conversion (Estimation of Performances in Periodically Oscillating Flow)," *International Journal of Rotating Machinery*, vol. 3, no. 4, pp. 233–238, 1997.
- [52] T. Setoguchi, K. Kaneko, H. Hamakawa, and M. Inoue, "Measurement of hysteresis on Wells turbine characteristics in reciprocating flow," in *Proceedings of the 1st International Symposium on Experimental and Computational Aerothermodynamics of Internal Flows*, pp. 537–543, 1990.
- [53] M. Inoue, K. Kaneko, T. Setoguchi, and H. Hamakawa, "Air turbine with self-pitch-controlled blades for wave energy generator," *JSME International Journal*, vol. 32, no. 1, pp. 19–24, 1989.
- [54] T. H. Kim, T. Setoguchi, K. Kaneko, and M. Takao, "The optimization of blade pitch settings of an air turbine using self-pitch-controlled blades for wave energy conversion," *Journal of Solar Energy Engineering*, vol. 123, no. 4, pp. 382–386, 2001.
- [55] K. Kaneko, T. Setoguchi, and S. Raghunathan, "Self-rectifying turbines for wave energy conversion," in *Proceedings of the 1st International Offshore and Polar Engineering Conference 1991*, vol. 1, pp. 385–392, 1991.
- [56] T. W. Kim, K. Kaneko, T. Setoguchi, and M. Inoue, "Aerodynamic performance of an impulse turbine with self-pitch-controlled guide vanes for wave power generator," in *Proceedings of the 1st KSME-JSME Thermal and Fluid Engineering Conference 1988*, vol. 2, pp. 133–137, 1988.
- [57] T. W. Kim, K. Kaneko, T. Setoguchi, E. Matsuki, and M. Inoue, "Impulse turbine with self-pitch-controlled guide vanes for wave power generator (effects of rotor blade profile and sweep angle)," in *Proceedings of the 2nd KSME-JSME Thermal and Fluid Engineering Conference 1990*, vol. 1, pp. 277–281, 1990.
- [58] T. Setoguchi, K. Kaneko, H. Maeda, T. W. Kim, and M. Inoue, "Impulse turbine with self-pitch-controlled guide vanes for wave power conversion: Performance of mono-vane type," *International Journal of Offshore and Polar Engineering*, vol. 3, no. 1, pp. 73–78, 1993.
- [59] T. Setoguchi, K. Kaneko, H. Maeda, T. W. Kim, and M. Inoue, "Impulse turbine with self-pitch-controlled guide vanes for wave power conversion," in *Proceedings of the 3rd International Offshore and Polar Engineering Conference 1993*, vol. 1, pp. 161–166, 1993.
- [60] H. Maeda, T. Setoguchi, K. Kaneko, T. W. Kim, and M. Inoue, "The effect of turbine geometry on the performance of impulse turbine with self-pitch-controlled guide vanes for wave power conversion," in *Proceedings of the 4th International Offshore and Polar Engineering Conference 1994*, vol. 1, pp. 378–382, 1994.
- [61] T. Setoguchi, K. Kaneko, H. Maeda, T. W. Kim, and M. Inoue, "Impulse turbine with self-pitch-controlled tandem guide vanes for wave power conversion," *International Journal of Offshore and Polar Engineering*, vol. 4, no. 1, pp. 76–80, 1994.
- [62] H. Maeda, T. Setoguchi, K. Kaneko, T. W. Kim, and M. Inoue, "Effect of turbine geometry on the performance of impulse turbine with self-pitch-controlled guide vanes for wave power conversion," *International Journal of Offshore and Polar Engineering*, vol. 5, no. 1, pp. 72–74, 1995.
- [63] T. Setoguchi, K. Kaneko, H. Taniyama, H. Maeda, and M. Inoue, "Impulse turbine with self-pitch-controlled guide vanes for wave power conversion: Guide vanes connected by links,"

- International Journal of Offshore and Polar Engineering*, vol. 6, no. 1, pp. 76–80, 1996.
- [64] T. Setoguchi, S. Santhakumar, H. Maeda, M. Takao, and K. Kaneko, “A review of impulse turbines for wave energy conversion,” *Journal of Renewable Energy*, vol. 23, no. 2, pp. 261–292, 2001.
- [65] K. Kaneko, T. Setoguchi, and S. Raghunathan, “Self-rectifying turbines for wave energy conversion,” *International Journal of Offshore and Polar Engineering*, vol. 2, no. 3, pp. 238–240, 1992.
- [66] M. E. McCormick and B. Cochran, “A Performance Study of a Radial Turbine,” in *Proceedings of the First European Wave Energy Conference 1993*, pp. 443–448, 1993.
- [67] M. E. McCormick, J. G. Rehak, and B. D. Williams, “An Experimental Study of a Bi-directional Radial Turbine for Pneumatic Energy Conversion,” in *Proceedings of the Mastering Ocean through Technology*, vol. 2, pp. 866–870, 1992.
- [68] T. N. Veziroglu, Ed., *Alternative Energy Sources VI, Wind/Ocean/Nuclear/Hydrogen*, vol. 3, Hemisphere Publishing Corporation, 1985.
- [69] T. Setoguchi, S. Santhakumar, M. Takao, T. H. Kim, and K. Kaneko, “A performance study of a radial turbe for wave energy conversion,” *Journal of Power and Energy*, vol. 216, no. A1, pp. 15–22, 2002.
- [70] M. Takao, Y. Fujioka, H. Homma, T. Kim, and T. Setoguchi, “Experimental Study of a Radial Turbine Using Pitch-Controlled Guide Vanes for Wave Energy Conversion,” *International Journal of Rotating Machinery*, vol. 2006, pp. 1–7, 2005.
- [71] T. Setoguchi, M. Takao, Y. Kinoue, K. Kaneko, S. Santhakumar, and M. Inoue, “Study on an impulse turbine for wave energy conversion,” *International Journal of Offshore and Polar Engineering*, vol. 10, no. 2, pp. 145–152, 2000.
- [72] A. El Marjani, F. Castro Ruiz, M. A. Rodriguez, and M. T. Parra Santos, “Numerical modelling in wave energy conversion systems,” *Energy*, vol. 33, pp. 1246–1253, 2008.
- [73] A. F. O. Falcão, L. M. C. Gato, and E. P. A. S. Nunes, “A novel radial self-rectifying air turbine for use in wave energy converters,” *Journal of Renewable Energy*, vol. 50, pp. 289–298, 2013.
- [74] A. F. O. Falcão, L. M. C. Gato, and E. P. A. S. Nunes, “A novel radial self-rectifying air turbine for use in wave energy converters. Part 2. Results from model testing,” *Journal of Renewable Energy*, vol. 53, pp. 159–164, 2013.
- [75] J. Lekube, A. J. Garrido, I. Garrido, E. Otaola, and J. Maseda, “Flow control in wells turbines for harnessing maximum wave power,” *Sensors*, vol. 18, no. 2, 2018.
- [76] A. J. Garrido, E. Otaola, I. Garrido et al., “Mathematical modeling of oscillating water columns wave-structure interaction in ocean energy plants,” *Mathematical Problems in Engineering*, vol. 2015, Article ID 727982, 11 pages, 2015.